Mixed Integer Linear Programming Path Planning of Autonomous Underwater Vehicles for Adaptive Sampling

Namik Kemal Yilmaz, Constantinos Evangelinos, *Member, IEEE*, Pierre F. J. Lermusiaux, Nicholas M. Patrikalakis, *Member, IEEE*,

Abstract

The goal of adaptive sampling in the ocean is to predict the types and locations of additional ocean measurements that would be most useful to collect. Quantitatively, what is most useful is defined by an objective function and the goal is then to optimize this objective under the constraints of the available observing network. Examples of objectives are better oceanic understanding, to improve forecast quality or to sample regions of high interest. This work provides a new path planning scheme for the adaptive sampling problem. We define the path planning problem in terms of an optimization framework and propose a method based on Mixed Integer Linear Programming (MILP). The mathematical goal is to find the vehicle path that maximize the line integral of the uncertainty of field estimates along this path. Sampling this path would improve the accuracy of the field estimates the most. While achieving this objective, several constraints must be satisfied and are implemented. They relate to vehicle motion, inter-vehicle coordination, communication, collision avoidance etc. The MILP formulation is quite powerful to handle different problem constraints and flexible enough to allow easy extensions of the problem. The formulation covers single and multiple vehicle cases as well as single and multiple day formulations. The need for a multiple day formulation arises when the ocean sampling mission is optimized for several days ahead. We first introduce the details of the formulation, then elaborate on the objective function and constraints, and finally present a varied set of examples to illustrate the applicability of the proposed method.

Index Terms

Autonomous Underwater Vehicle, AUV, path planning, trajectory planning, mixed integer linear programming based path planning, adaptive sampling, AOSN, data assimilation, error subspace,ocean modeling, Monterey Bay.

I. Introduction

REAL-TIME ocean forecasting is a challenging task due to issues which involve the intermittent nature of the ocean, the practical inability to make extensive and sustained in-situ measurements, the uncertainties in the initial and boundary conditions, and the limited information at depth to complement the satellite measurements. In order to accurately forecast the evolution of a complex system as the ocean, one needs to take into account the possibly large deviations of the solution due to small initial and boundary uncertainties [1]–[4]. Weather and ocean forecasts also suffer from intrinsic uncertainties which arise due to errors in the model formulation and errors in its numerical solution. Finally, even if one could uniformly sample the ocean, much of the data corresponding to regions of low dynamical variability would be redundant while data pertaining to regions of high dynamical variability would be lacking resolution. Therefore, to utilize the measuring assets in an optimal way, one must plan ahead the sampling strategy to be followed. Our work describes, implements, illustrates and evaluates new technical schemes for the optimal planning of the path of ocean platforms based on Mixed Integer Linear Programming and advanced uncertainty estimates for ocean prediction.

Observation networks used for weather and ocean forecasting can be thought of being composed of a routine and an adaptive component [5]. The routine component comprises observations from the fixed observing network, satellite measurements and other measurements that are routinely taken. The routine

Manuscript received ?; revised ?

component collects the data that is situation-independent. An additional component can be utilized to collect more data in regions critical to a specific objective. This objective is often a function of the synoptic oceanic or atmospheric dynamics and variability. The additional network component thus needs to be adaptive because the form of the objective can be modified but also because the fields to be measured are dynamic. For example, for adaptive sampling on the daily time scale, the critical regions to be measured can be expected to vary from day to day. In the ocean, the adaptive component might involve ships or (un)-manned aircrafts which drop instruments in data-sensitive regions, autonomous underwater vehicles (AUVs), gliders, etc. In an ocean estimation problem, measurements can impact both past and future field estimates as a function of advection, diffusion and other ocean processes. The adaptive network can then be continually directed to locations which maximize the expected improvements in some aspect of the estimation. This problem is known as *targeting*, *adaptive observations* or *adaptive sampling* [6]–[8].

Adaptive sampling can serve several purposes and have different forms. When scarcity of measurement assets exists, the whole routine component can also be treated as an adaptive network. Adaptive observation schemes have several goals, such as decreasing the uncertainty, gathering critical information about the dynamics of the system, increasing the coverage of the system, etc. An important goal is to increase the accuracy of the estimates of the states of interest by utilizing the resources at hand in an optimal manner. The estimates can be the (i) nowcast fields, e.g. determine the data needed now to best improve current estimates; (ii) forecast fields, e.g. determine the data needed before the target prediction that will best improve this prediction; or, (iii) the past fields, e.g. determine the data that will minimize errors in the initial conditions.

A variety of techniques have been employed to determine the ideal location of extra observations within an adaptive sampling network. Since the goal is to combine data and models, most are based on data assimilation approaches [9]. These techniques include singular vector technique [10]–[13], the analysis sensitivity technique [14], the observations technique [15], the ensemble transform (ET) technique [3], the Kalman filter technique [16], the ensemble transform Kalman filter (ETKF) technique [5], [17] and the nonlinear error subspace statistical estimation technique (ESSE) [6], [18]–[20].

Although all these techniques are very useful in different ways to distinguish potential regions for extra observations, they do not intrinsically provide a path for the adaptive platforms. Path planning of the adapftive elements for the network is often performed based on predesigned tracks as explained for example in [17], [19], [20]. As the size of the adaptive network grows, the complexity of the routing problem gets amplified and the lack of rule-based path planning schemes can lead to sub-optimal plans.

Although adaptive sampling is now becoming an active research area, rule-based high level path planning for oceanic adaptive sampling has not yet received a lot of attention. Previous work in environmental path generation includes path planning for atmospheric networks [17], [12], which can have quite different considerations than an ocean network including assets like AUVs and internal ocean dynamics at mesoscales which are usually slower than weather scales. In ocean adaptive sampling, the body of previous work involve low level path planning, control and coordination issues. The commonality of these approaches is that either waypoints are given a priori or that simple and local search techniques such as gradient methods (greedy search) are employed to locate the waypoints [21], [17]. The use of such local techniques is useful and promising, but it does not guarantee global optimality.

Optimal sampling algorithms with similarities to ours have been used in other scientific and engineering domains, but often with different objectives, constraints and types of asset behaviour. Such algorithms and approaches include the Selective Traveling Salesman Problem (STSP), routing problems and some particular path planning problems [22], [23], [24], [21], [25], [26]. In STSP, there are nodes with some award points associated to them. Given a limited travel time, the aim is to collect as much reward as possible. Unlike the classic Traveling Salesman Problem (TSP), not all the nodes need to be visited. Only the most rewarding nodes are to be targeted. In the ocean, the existence of many geometrical and operational constraints, and the fact that the terminal location of the vehicle is unknown at the beginning of the problem, make the path generation problem remarkably different and more difficult than STSP. Recent research exists on path planning and coordination issues of Unmanned Aerial Vehicles (UAV)

[25], [26] which present a good insight to the use of MILP in path planning. Collecting rewards along the paths of the vehicles in our case corresponds to taking line integrals along each paths. Another difference is the lack of waypoint information in our case.

In what follows, we first lay out the problem statement (Sect. 2) and develop and determine the objective function (Sect. 3). We then formulate a set of motion constraints (Sect. 4) and present af solution method for the optimum generation of the observational paths. We carry out a series of examples, with single time cases (Sect. 6) and multiple time situations (Sect. 7). We conclude with Sect. 8.

II. Problem Statement

To carry out adaptive sampling, we first need a field that ranks and locate the regions of interest. These regions may be characterized by using the uncertainty predictions on the states (error variances, PDFs, etc..) or physical features of dynamical interest (eddies, upwelling, jets, etc..). The former one is a vector or a scalar field (continuous in time and space) provided by the Harvard Ocean Prediction System (HOPS) and Error Subspace Statistical Estimation (ESSE) system ([27]–[29]), whereas the latter is a set of sub-regions which needs to be selected manually or directly detected using feature extraction ([30], [31] and possibly presented as a Boolean field (e.g. discontinuous field). Since information from both sources is valuable, it is advantageous to combine the two sources of information. This involves the investigation of an optimal way to merge two different requirements into a single field [32]. In this study, it is assumed that such a combined field is given. The methods developed and implemented are independent of the type of fields. For the examples provided, the fields used are uncertainty information on ocean states provided by ESSE/HOPS, which we refer to as ”uncertainty fields”.

The uncertainty field is representative of the location of observation points to be targeted. For a nowcast, high uncertainty values correspond to the coordinates that are primarily worth visiting. The oceanographic assets that are generally available for sampling include buoys, Autonomous Surface Crafts (ASCs), Autonomous Underwater Vehicles (AUVs), gliders and oceanographic ships which can be utilized also to deploy the AUVs. In this study, we focus on the path planning problem for AUVs which is sufficiently generic to also allow the solution of sampling problems with other available assets.

The problem at hand is a constraint-optimization problem. The objective is to sample the regions of greatest uncertainty. For a group of assets (AUVs), it can be stated as finding the optimal sampling patterns/routes within the specified constraints (vehicle motion, inter-vehicle coordination, communication, collision avoidance) such that the total observational gain during the travel of the assets is maximized. By observational gain we mean the uncertainty values. The complete picture of the problem is obtained when multiple time scales are considered. A standard ocean approach to adaptive sampling has been to consider the nowcast problem and to construct the observational waypoints or paths on a day-by-day basis. For planning further ahead in time, one approach is to treat the optimization problem in an inter-temporal manner. In generating an AUV path over 2 days, tomorrow’s starting point is then related to today’s endpoint. Instead of a myopic approach, coupling the paths belonging to consecutive days allows a more far-sighted optimality. This requires of course that an estimate of the uncertainties on the state estimates is available for each day in our targeted timescale. In general, adaptive sampling paths can be planned for as far ahead in time as the time for which the fields of interest are predictable.

If the physical sampling optimized by the present approach is carried out, the data collected is utilized, either on its own or is assimilated in ocean models for optimal field estimation. This is what is being simulated in this paper. In all cases, the data or the data-driven model estimates can be utilized for scientific studies and societal applications. We refer for example to [4], [9].

Inputs to the problem are here chosen to be the uncertainty fields and the unknowns in the problem are the x and y coordinates of the paths of each vehicle involved in the problem. The path of p^{th} vehicle is discretized into $N_p - 1$ segments by using N_p points and assigned variables that stand for x and y coordinates. Then with the desired objective function and proper problem constraints, the optimizer is expected to solve for the x and y coordinates for each discrete waypoints. The path is constructed by

connecting consecutively numbered points. The lower and the upper limit on the x and y values are determined by the coordinates of the terrain under consideration. This framework is depicted in Fig 1(a). The starting point of motion which is supplied as the initial condition to the system is shown by a white dot. The black dot denotes the terminal point, and the grey dots show the intermediate points.

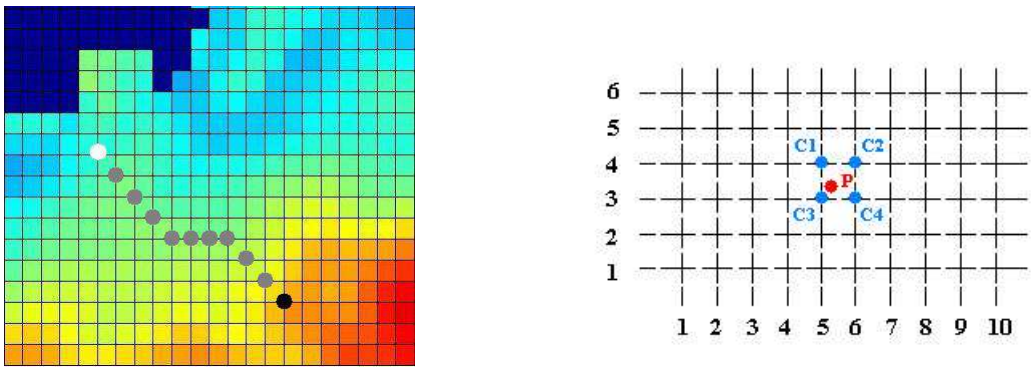

(a) (b)

Fig. 1. a) Path construction by segmentation. b) Representation of value at any coordinate as a convex combination of the values of four neighboring grid points.

III. Objective Function

In a $2D$ discrete scenario for a single vehicle, the objective function can be written as:

$$max \sum_{i=1}^{N} P(x(i), y(i)) \tag{1}$$

where P stands for the $2D$ array that represents the uncertainty field and $x(i)$ and $y(i)$ represent the x and y coordinate values of the i^{th} point on the path. In the single-vehicle case x and y are vectors of length N. $x(1)$ and $y(1)$ correspond to the starting point coordinates and are input to the system. The rest of the x and y vectors are unknowns.

In general the uncertainty fields are neither convex nor concave functions. The field characteritics requires the use of piecewise curve fitting to properly represent the field. We chose to use linear piecewise curve fitting for our formulation purposes. In an optimization formulation framework this is facilitated by the use of special ordered set (SOS) of type 2. An $SOS2$ is a set of continuous or integer variables among which only two variables *can* be non-zero. Also the two nonzero variables *must* be adjacent in the ordering assigned to the set. Using $SOS2$ functionality it is possible to approximate a non-convex, non-concave $2D$ nonlinear function such as Equation 1. This concept is first introduced by Beale and Tomlin [33] and have been developed by H.P. Williams. We refer to [34] for a detailed discussion of the topic.

Let U_{ij} denote the values of the function $z = f(x, y)$ on the computational 2D grid. The grid spacings do not need to be equidistant. Any given function $z = f(x, y)$ can be approximated by the following equations:

$$\sum_i DX_i \cdot lx_i \quad is \quad sos2 \tag{2}$$

$$\sum_j DY_j \cdot ly_j \quad is \quad sos2 \tag{3}$$

where lx and ly are arrays that correspond to unknown weights at the integer x and y coordinates over which function $z = f(x, y)$ is defined. DX and DY are arrays of integers that define the range of the x and y coordinates of the given U_{ij}, respectively. Their elements are equated to the corresponding index ($DX_i = i, DY_j = j$). They are used to weave the grid region under consideration When we define $\sum_i DX_i \cdot lx_i$ to be SOS2, it means that, in the output set only two adjacent element can be nonzero.

$$\sum_j lxy_{ij} = lx_i \quad \forall i \tag{4}$$

$$\sum_i lxy_{ij} = ly_j \quad \forall j \tag{5}$$

lxy is a weight matrix. lxy_{ij} stands for the weight at a specific integer point coordinate and is a function of lx and ly . lx, ly and lxy are all unknown variables in the formulation. These "auxiliary" variables are dependent of the targeted x, y values and will be determined accordingly. Equations 4 and 5 establish the conservation of weight along each row and column.

$$\sum_i lx_i = 1 \tag{6}$$

$$\sum_j ly_j = 1 \tag{7}$$

Equations 6 and 7 enforces convexity. For a non-integer coordinate, this condition guarantees that the corresponding z value will be a convex combination of that of two or four neighboring integer coordinates.

To exemplify, for the field presented in Fig 1(b), DX contains the values of $1, 2...10$ and DY the values $1, 2...6$. The first $SOS2$ condition states that the multiplication of lx with DX will create a set of numbers such that at most two elements in the set could be non-zero and they must be adjacent. If one calculates $f(3.5, 5.5)$, this condition ensures that only the elements corresponding to $x = 3$ and $x = 4$ in the set should turn out to be non-zero. A similar argument is true for the y coordinate. As a result, at most 4 elements in both direction might come out to be non-zero and the values of U_{xy} corresponding to these four coordinates will be used to approximate the value of $f(x, y)$ at a non-integer coordinate.

Then x, y and f can be calculated using

$$x = \sum_i DX_i \cdot lx_i \tag{8}$$

$$y = \sum_j DY_j \cdot ly_j \tag{9}$$

$$f = \sum_i \sum_j U_{ij} \cdot lxy_{ij} \tag{10}$$

In conjunction with the other constraints added, the optimal values of x and y and resulting value of function f will be fixed to satisfy the given objective function.

The above discussion lays the foundation for representing the nonlinear field and the above formulation is good for finding the value at a single (x, y) coordinate. In our problem however, the path is segmented by N points and the above formulation should be carried out at each path point. In the case of multi-vehicles, every path point belonging to each vehicle needs to be accounted for. For these extensions to the multi-vehicle and multi-coordinate case, one simply adds additional indices to the notation introduced above. The reader can see [35] for further details.

The objective is to maximize the summation of line integrals of the uncertainty values along the path of each vehicle in the fleet. The objective function can be written as:

$$max \sum_{p=1}^{P} \sum_{k=1}^{N_p} f_{pk} \tag{11}$$

where P is the total number of vehicles in the fleet and N_p is the total number of path-points belonging to the p^{th} vehicle. In all of the above equations, subscripts p and k stand to denote the k^{th} path-point of p^{th} vehicle. U_{ij} (which is composed of the discretized values of the function $z = f(x, y)$ on the computational 2D grid) stands for the uncertainty field data which is the input to our problem.

IV. Motion Constraints

For the vehicles to move in a desired manner, some constraints that shape the vehicle navigation are needed: primary motion, anti-curling, vicinity, communications and obstacle avoidance constraints.

A. Primary Motion Constraints

When the vehicle is at a particular path-point except the terminal point, it needs to move to the next path-point. A constraint is thus needed to thrust the vehicle to the next path-point. Referring to Figure 2(a), if the vehicle is at the blue point numbered as 1, it can only move to one of the 8 adjacent points shown in green.

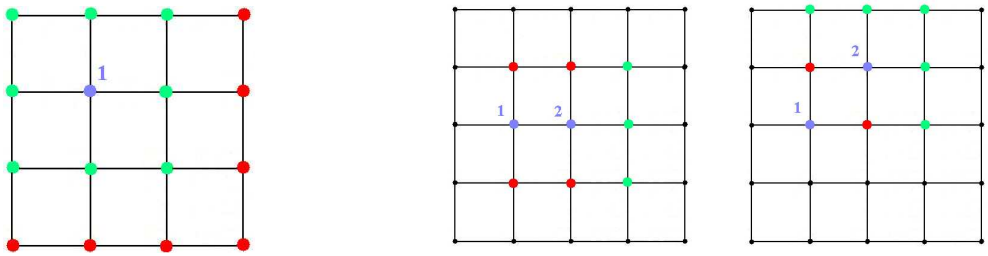

(a) (b)

Fig. 2. a) Allowable set of path-points by taking into account the spatial constraints between the candidate point and the point that precedes it by one. Blue dots represent current path-points in the path, green ones show the allowable path-point locations and the red ones show the unallowable path-point locations for the path-points under consideration. b) Allowable set of path-points by taking into account the spatial anti-curling constraints between the candidate point and the point that precedes it by two. Blue dots represent current path-points in the path, green ones show the allowable path-point locations and the red ones show the unallowable path-point locations for the path-points under consideration.

Explained motion can be achieved by the following set of constraints:

$\forall p \in [1, ..., P], and \quad \forall i \in [2, ..., N_p]$:

$$x_{pi} = x_{p(i-1)} + b_{pi1} - b_{pi2} \tag{12}$$

$$b_{pi1} + b_{pi2} \leq 1 \tag{13}$$

$$y_{pi} = y_{p(i-1)} + b_{pi3} - b_{pi4} \tag{14}$$

$$b_{pi3} + b_{pi4} \leq 1 \tag{15}$$

$\forall p \in [1, ..., P], and \;\; \forall i \in [2, ..., N_p]$:

$$b_{pi1} + b_{pi2} + b_{pi3} + b_{pi4} \geq 1 \tag{16}$$

$\forall p \in [1, ..., P], \quad \forall i \in [2, ..., N_p], and \;\; \forall j \in [1, ..., 4]$:

$$b_{pij} \in 0, 1 \tag{17}$$

The $b_{pi1}, b_{pi2}, b_{pi3}$ and b_{pi4} in Equations 12–17 are auxiliary binary variables needed to model the propulsive motion constraint. If b_{pi1} is set to 1 and b_{pi2} is set to 0 then the x-coordinate of the next path-point will be one unit greater than that of the current one and similarly for the y-coordinate. If they are both set to zero it means that the x-coordinate should not change, which is an allowable possibility. Another scenario that will keep the x-coordinate fixed is when both b_{pi1} and b_{pi2} are set to 1. This is a degenerate case and it must be avoided. To ensure both b_{pi1} and b_{pi2} will not be set to 1 at the same time, Equation 13 is introduced. A similar argument follows for the y-coordinate, see Equations 14 and 15. To avoid the vehicle get stuck at the same x and y coordinates Equation 16 is included.

B. Anti-Curling/Winding Constraints

When a point in the map is visited and measurements are made, not only the uncertainty value at the particular point but also the uncertainty value at the neighboring points are decreased, due to correlations among ocean values. Therefore there exists an area of influence for a measurement. If the vehicle curls around the same area too much, it will be visiting points whose uncertainty values are already decreased by previous measurements. This results in inefficient consumption of range. To introduce correlations along the vehicle paths, we relate the coordinates of a path-point to these of the path-point preceding it by two path-points, to the coordinates of the path-point preceding it by three path-points, and so on up to the desired point depending on given range value. The parameters in this approach can adjust the straightness/curvature of the path, as desired.

The first set of constraints that will be imposed to straighten the path, involves the relative location of the x and y coordinates of a path-point with respect to the x and y coordinates of the path-point that precedes it by two. These constraints can be described as follows:

$\forall p \in [1, ..., P] \;\; and \;\; \forall i \in [3, ..., N_p]$:

$$|x_{pi} - x_{p(i-2)}| \geq \Delta_1 \;\; \textbf{OR} \;\; |y_{pi} - y_{p(i-2)}| \geq \Delta_1 \tag{18}$$

In this formulation Δ_1 is a design parameter and can be adjusted to create the desired path straightness as described before. A possible choice of Δ_1 for the kind of field sizes and ranges we deal with is 2. Figure 2(b) depicts some allowable move scenarios. Blue dots numbered as 1 and 2 are the two preceding path-points. The red dots show unallowed moves. The green dots show the allowable locations for the next path-points. These choices of allowable path-points are generated by aggregately taking into account the previous propulsive constraints.

But Equation 18 is a nonlinear constraint and must be transformed into a linear one in order to be used in a *Mixed Integer Linear Program* (MILP). This transformation will be done in two steps. First, the absolute value constraint can be eliminated by the following transformation:

$\forall p \in [1, ..., P] \;\; and \;\; \forall i \in [3, ..., N_p]$:

$$\begin{aligned} & x_{pi} - x_{p(i-2)} \geq \Delta_1 \\ or \quad & x_{p(i-2)} - x_{pi} \geq \Delta_1 \\ or \quad & y_{pi} - y_{p(i-2)} \geq \Delta_1 \\ or \quad & y_{p(i-2)} - y_{pi} \geq \Delta_1 \end{aligned} \tag{19}$$

Equation 19 is a disjunctive constraint and is not a suitable kind of constraint for a MILP formulation. Constraints in a MILP formulation must be conjunctive. It is possible to transform a disjunctive constraint into a conjunctive one by using auxiliary binary variables and "Big-M" constants [36]. Such transformation yields:

$\forall p \in [1, ..., P] \quad and \quad \forall i \in [3, ..., N_p]$:

$$\begin{aligned} & x_{pi} - x_{p(i-2)} \geq \Delta_1 - M * t1_{pi1} \\ and \quad & x_{p(i-2)} - x_{pi} \geq \Delta_1 - M * t1_{pi2} \\ and \quad & y_{pi} - y_{p(i-2)} \geq \Delta_1 - M * t1_{pi3} \\ and \quad & y_{p(i-2)} - y_{pi} \geq \Delta_1 - M * t1_{pi4} \end{aligned} \tag{20}$$

$$and \quad \sum_{w=1}^{4} t1_{piw} \leq 3 \tag{21}$$

$$t1_{piw} \in 0, 1 \quad \forall w \in [1, ..., 4] \tag{22}$$

the numbers that may appear on any side of the inequalities.

As a variation of the same theme, the second set of constraints that will be imposed to straighten the path involves the relative location of the x and y coordinates of a path-point with respect to the x and y coordinates of the path-point that precedes it by two. These constraints can be written as follows:

$\forall p \in [1, ..., P] \quad and \quad \forall i \in [4, ..., N_p]$:

$$|x_{pi} - x_{p(i-3)}| \geq \Delta_2 \quad \textbf{OR} \quad |y_{pi} - y_{p(i-3)}| \geq \Delta_2 \tag{23}$$

For example, consider Δ_2 set to 2.5. Figure 3(a) shows some allowable move scenarios. As before, the constraint presented by Equation 23 combines with the other motion constraints: the allowable moves presented in Figure 3(a) are a result of the collective restrictions on the navigation of the vehicle. Blue dots numbered as 1, 2 and 3 are the three preceding path-points.

Equation 23 can be transformed into an MILP formulation as explained above. The reader can see [35] for further details.

This approach can be extended to include the relation between more path-points in a row to avoid curling that depends on the range of the vehicle and the features of a given field. The allowed minimum curvature can be estimated as the average of $Delta_1$ and $Delta_2$.

C. Vicinity Constraints for Multi-Vehicle Case

In the case in which there exist multiple vehicles navigating to different regions of the mission zone, first and foremost collisions between vehicles must be avoided. In any case, as discussed for the curling constraint, it is also disadvantageous for two vehicles to navigate too close to each other, even if they do not run the risk of colliding. In the case of multiple peaks and available vehicles starting their motion

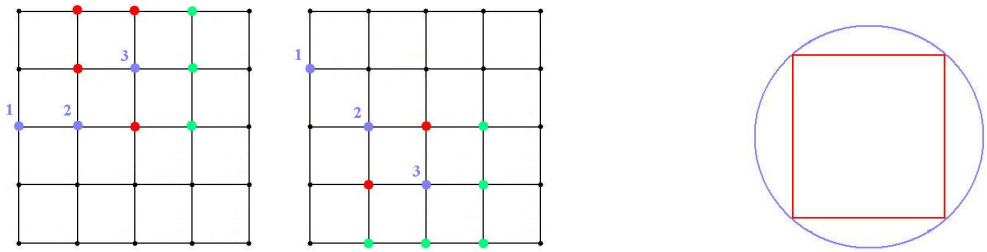

(a) (b)

Fig. 3. a) Allowable set of path-points by taking into account the spatial anti-curling constraints between the candidate point and the point that precedes it by three. Blue dots represent current path-points in the path, green ones show the allowable path-point locations and the red ones show the unallowable path-point locations for the path-points under consideration. b) Approximation of a circle by a square.

close to the stronger peak, the vicinity constraints can help vehicles get separated. Anti-vicinity constraint can thus, as a result, lead to the visiting of some weaker peaks further away and which would not be visited otherwise.

To achieve this, for every pair of vehicles p and q, every pair of path-points must be a safe distance apart from each other. Let the safety distances in x and y directions be denoted by Δx_{safety} and Δy_{safety} respectively. The vicinity constraints then can be constructed as follows:

$\forall p, q \in [1, ..., P] : \forall p, q | \, p > q \; ; \quad \forall i, j \in [1, ..., N_p] :$

$$|x_{pi} - x_{qj}| \geq \Delta x_{safety} \quad \textbf{OR} \quad |y_{pi} - y_{qj}| \geq \Delta y_{safety} \tag{24}$$

Utilizing the transformations to handle the absolute value and the conjunctive constraints as elucidated in the previous subsection, Equation 24 can be expanded into an MILP formulation. The reader can see [35] for further details. Again Δx_{safety} and Δy_{safety} are design parameters and can be varied depending on the field features, number of vehicles and vehicle range.

D. Coordination Issues Related to Communication with AUV

There exist few different scenarios related to the communication issues and they are discussed below: AUV-ship, AUV-shore and AUV-network communications [37], [38], [39].

1) Coordination with a Ship and ship shadowing: . The nature of our adaptive sampling problem can still often utilize a ship to move with the AUV fleet, so as to facilitate at-sea launch and retrieval of AUVS as well as fast transit and AUV battery recharge. In general, the AUV can communicate with the ship for data transmission. Inclusion of a ship in the adaptive network enables to visit locations far from the shore stations and perform *broad-area coverage* problems [21]. The ship AUV coordination issue adds another dimension to the problem. The ship and the AUVs in the fleet that are linked to the ship must navigate in harmony to finish the mission successfully. When the mode of communication is brought into consideration, there emerge three cases to consider. The first one is communication via acoustical means, second is radio communication or direct link.

Acoustic Communication. For an acoustic link to work [40], [41] during the mission the AUV must stay in the vicinity of the ship. In addition to that when its charge is consumed it must either return to the ship or park at a surface location that is close enough to be picked up by a boat dispatched from the ship. To impose this characteristic to the AUV motion we need to add some extra constraints. The end point of the

AUV can either be specified to be the coordinate of the ship, or stay in the same vicinity of the vehicle as the rest of the path-points, or it can be dictated that although it does not need to be same as the ship coordinates (meaning return to the ship) it should be closer to the ship than the rest of the path-points. Also in order to synchronize the motion of the ship and the AUV fleet the path of the ship must be known. Once the ship path is known (ship path can be determined using ideas and methods similar to the ones presented in this paper) it can be segmented into as many path-points as the AUV. Then, the time domain dependence is unique between identically indexed ship and AUV path points. The n^{th} path-point of the ship then corresponds to the location of the ship when the AUV visits its n^{th} path-point. If all AUVs in the fleet have same number of path-points, a single segmentation is enough, if they do not then the ship path segmentation must be performed for every AUV. Assuming that the terminal path-point of the AUV stays within the same distance to the ship as the other path-points, these ideas can be put into MILP formulation as follows:

$\forall p \in [1, ..., P] \quad \forall i \in [1, ..., N_p]$:

$$\begin{aligned} |x_{pi} - ship\_x_{pi}| \leq \Delta x_{ship\_vicinity} \quad \textbf{AND} \\ |y_{pi} - ship\_y_{pi}| \leq \Delta y_{ship\_vicinity} \end{aligned} \tag{25}$$

where $ship\_x_{pi}$ and $ship\_y_{pi}$ stand for x and y coordinates of the i^{th} path-point of the ship path segmentation for p^{th} vehicle. $\Delta x_{ship\_vicinity}$ and $\Delta y_{ship\_vicinity}$ are the constants that are used to define region of vicinity for a ship. The region of coverage can be thought of as a circle centered at the coordinate of the ship. Equation 26 approximates this circular region by a square for the sake of simplicity of formulation. This is shown in Figure 3(b).

A more complex alternative to define this region is to approximate a circle by the biggest polygon that will fit inside the circle and write down the equations of lines that construct the polygon with q edges as a function of coordinates of the i^{th} path-point of p^{th} vehicle. The constraint set is formed by adding inequalities either of type $a_{piq}x + b_{piq}y \leq c_{piq}$ or of type $a_{piq}x + b_{piq}y \geq c_{piq}$, depending on the equation in consideration. This imposes the confinement of the (x, y) point inside the hexagon. As explained before Equation 26 can again be transformed into an MILP The above equation can be transformed into an MILP formulation. The reader can see [35] for further details.

a) Another issue that arises in ship AUV coordination is the collision avoidance between the AUVs and the ship. This condition can be met by introducing a minimum safety distance between the ship and the AUVs that must be observed during the course of the sampling. Extending the previous idea, this condition can be formulated as follows:

$\forall p \in [1, ..., P] \quad \forall i \in [1, ..., N_p]$:

$$|x_{pi} - ship\_x_{pi}| \geq \Delta x_{ship\_safety} \quad \textbf{OR} \tag{26}$$

$$|y_{pi} - ship\_y_{pi}| \geq \Delta y_{ship\_safety} \tag{27}$$

The above equation can be transformed into an MILP formulation as explained above. The reader can see [35] for further details.

b) To handle the cases where the terminal path must be in a tighter vicinity of the vehicle or the AUV must return to the ship, the constraints that account for terminal path-point must be specially treated. If an AUV is to return to the ship, we can have the extra constraint:

$$x_{pN_p} = ship\_x_{pN_p} \quad \forall p \in [1, ..., P]$$
$$y_{pN_p} = ship\_y_{pN_p} \quad \forall p \in [1, ..., P] \tag{28}$$

c) Or if the terminal path-point needs to lie in a tighter vicinity than the other path-points for the ease of picking up, then we need to add the constraints:

$\forall p \in [1, ..., P]$:

$$|x_{pN_p} - ship\_x_{pN_p} \leq \Delta x_{ship\_vicinity\_TP} \quad \textbf{OR}$$
$$|y_{pN_p} - ship\_y_{pN_p} \leq \Delta y_{ship\_vicinity\_TP} \tag{29}$$

where $\Delta x_{ship\_vicinity\_TP}$ and $\Delta y_{ship\_vicinity\_TP}$ stand for the tighter bounds on the vicinity of terminal path-points to the ship. The above equation can be transformed into an MILP formulation as explained above. The reader can see [35] for further details.

Radio and direct communications. As aforementioned, the two other alternatives for communication are the radio link and the direct communication. If the preferred way of communication is opted to be wireless communication (radio) the AUV needs to be in some vicinity of the ship at the end of its motion to communnicate with the ship. In that case only the Equation 29 needs to apply.

If direct connection is the selected communication method, the AUV needs to board the ship at the end of the mission and in which case, only Equation 28 needs to be applied.

2) Communication with a Shore Station: In the case of shore station, the end path-point coordinates of the vehicles need to either lie in a vicinity of the station location to establish radio communication or they must match with the coordinates of the shore station if they are required to return to it. If the vehicles need to lie in a proximity of the shore station to be picked up by a boat, we need to introduce the constraints:

$\forall p \in [1, ..., P]$:

$$x_{pN_p} - shore\_x \leq \Delta x_{shore\_vicinity} + M * s3x_{p1}$$
$$and \quad shore\_x - x_{pN_p} \leq \Delta x_{shore\_vicinity} + M * s3x_{p2}$$
$$and \quad y_{pN_p} - shore\_y \leq \Delta y_{shore\_vicinity} + M * s3y_{p1}$$
$$and \quad shore\_y - y_{pN_p} \leq \Delta y_{shore\_vicinity} + M * s3y_{p2} \tag{30}$$
$$and \quad \sum_{w=1}^{2} s3x_{pw} \leq 1 \tag{31}$$
$$and \quad \sum_{w=1}^{2} s3y_{pw} \leq 1 \tag{32}$$

$$s3x_{pw}, s3y_{pw} \in 0, 1 \quad \forall w \in [1, ..., 2] \tag{33}$$

where, $shore\_x$ and $shore\_y$ stand for the x and y coordinates of the shore station. Or, if the vehicle needs to return to the shore station, one can impose:

$$\begin{aligned} x_{pN_p} &= shore\_x \quad \forall p \in [1, ..., P] \\ y_{pN_p} &= shore\_y \quad \forall p \in [1, ..., P] \end{aligned} \tag{34}$$

3) Communication with an AOSN: The communication with buoys comes into play in the context of an *Autonomous Ocean Sampling Network (AOSN)*, (http://www.mbari.org/aosn/default.htm), [42]. AOSN research is still very active. The main goal is to realize a completely autonomous network that efficiently collects data from the ocean. The network consist of AUVs, buoys, shore stations, acoustic modems, satellite and radio links and any other potential autonomous vehicles such as gliders. In one scenario, the shore station makes the mission plan and sends it to the buoys via a radio link. Buoys establish an acoustical communication link with AUVS and upload the individual path plans to the AUVs. The AUVs navigate in accordance to the uploaded plan and make necessary measurements. When the mission is over the collected data is transmitted to one of the buoys from which data is sent to the shore station using the wireless connection. Also, buoys not only act as an intermediate data logger but also as docking stations where AUVs can be recharged and continue their mission without the need to be carried to shore or to a ship. Figure 4 illustrates an AOSN.

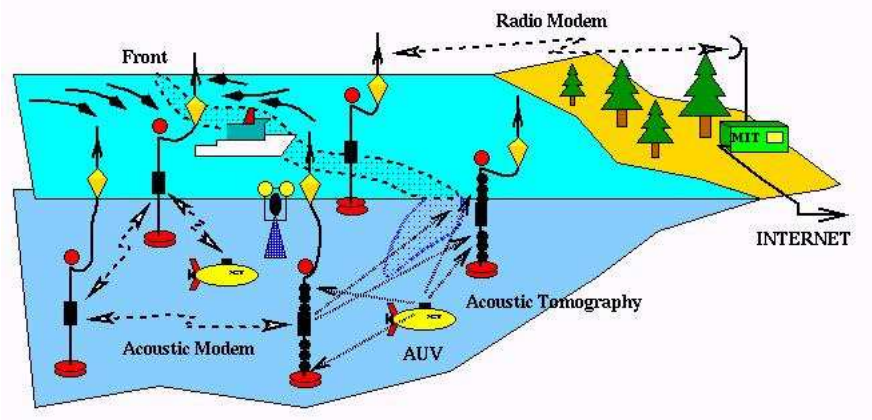

Fig. 4. Illustration of an "Autonomous Oceanographic Sampling Network" [43].

Even though a few large scale projects on AOSN have occurred or are underway, a complete and efficient physical implementation of a truly autonomous AOSN has not yet been realized. For example, a missing component has been a fully automated and sustained path planning. Nonetheless, we can still offer a formulation hinging around an extended functionality of buoys as docking stations in addition to being a node in the communication network. If we consider a single day mission, we can introduce the condition that the AUV must return to the closest buoy at the end of the day and if we assume we have M buoys whose coordinates are represented by the arrays $buoy\_x_h$ and $buoy\_y_h$, we can write:

$\forall p \in [1, ..., P]$:

$$x_{pN_p} = \sum_{h=1}^{M} buoy\_x_h * bv_{ph}$$

$$y_{pN_p} = \sum_{h=1}^{M} buoy\_y_h * bv_{ph} \tag{35}$$

$$\sum_{h=1}^{M} bv_{ph} = 1 \qquad \forall p \in [1, ..., P] \tag{36}$$

$$bv_{ph} \in 0, 1 \quad \forall h \in [1, ..., M] \tag{37}$$

Variables bv_{ph} are auxiliary variables that help to choose one of the buoy coordinates as the end point coordinate of AUVs. Equation 36 guarantees that only one buoy coordinate will be assigned to a specific AUV. Also depending on the docking capabilities of an buoy we can impose the constraint that at most one AUV can park at a given buoy. This can be formulated as:

$$\sum_{p=1}^{N} bv_{ph} \leq 1 \qquad \forall h \in [1, ..., M] \tag{38}$$

Other constraints related to the communication with buoys or some other constraint that cannot be foreseen at this time without an actual implementation of an AOSN might need to be added. Given the flexibility and strength of the suggested formulation framework, other requirements that could emerge depending on the specific implementation of an AOSN can easily be added to the formulation.

E. Obstacle Avoidance

In the case of existence of obstacles in the region of interest, the task of collision prevention with obstacles could be managed in two alternative ways. One option is to introduce inequalities which will remove the regions where obstacles lie from the feasible coordinate set of the vehicle navigation. Another, simpler approach is to set the uncertainty values within the regions occupied by the obstacles to a very large negative number. Those points will not be included in the solution since their inlusion will have negative contribution to the objective function. For other approaches on obstacle avoidance, we refer to [44], [45], [46], [47].

V. Methodology and Software Selection for the MILP Solution

Our choice of implementation platform is XPress-MP optimization package from “Dash Optimization” (http://www.dashoptimization.com). It has a MILP solver which uses brand and bound algorithm. It is suitable for solving our path planning problem.

For optimum performance and ease of development, the ideal is to use a high level modeling language that is compatible with the solver. Such modeling languages are especially made for optimization problems and are equipped with powerful tools to implement optimization problems faster. A modeling language offered by Dash Optimization is *Mosel*. Implementing the mathematical program in *Mosel* is straightforward, requiring minimal translation from the canonical form shown in Equations 2–38. Also, *Mosel* is capable of easily implementing the $SOS2$.
constraints.

VI. Results for Single-Day Case

Our methodology and software have been tried on a wide variety of different scenarios with multiple types of fleet sizes, ranges, starting points and constraints. The ocean fields that have been used are the temperature forecast uncertainty maps in Monterey Bay during August-September 2003, as calculated by the Harvard Ocean Prediction System (HOPS) and Error Subspace Statistical Estimation (ESSE) system (see Sect 2). In the examples that follow, most examples shown are for August $27, 2003$ and utilize uncertainty averages from the upper $[0-40]$m ocean layers, focusing on largest uncertainties in the ocean surface mixed-layer and ocean thermocline dynamics. Depending on the objective, velocity or salinity fields (or even a weighted average of all fields) can also be used with our software.

In all of the following graphs grey dots indicate the starting point of the motion, white dots indicate the final point on the path. One important parameter in the problem formulation that controls the range for a given vehicle is the number of path-points, "N_p". It is not directly equal to the range since diagonal moves are allowed. Its value must be chosen based on the allowable range for each AUV on a given day. Once the problem is solved with the initial selection for "N_p", depending on the length of the generated path, some iterations might be necessary.

A. Results for Single-Vehicle Case

In this sub-section we look at look at an example where we have a single vehicle. Figure 5(a) presents the path generated for a vehicle, given the starting coordinates and number of path points as the input along with the uncertainty field. As it can be seen on this Figure 5(a), the generated path successfully covers the regions of high uncertainty. To illustrate the solution time as a function of range, the same problem is solved for different path ranges. The result is presented in Figure 5(b) which reveals that the solution time increases exponentially as a function of vehicle range. This behavior is expected since the formulation is a binary integer program and binary integer programs are known to be NP hard.

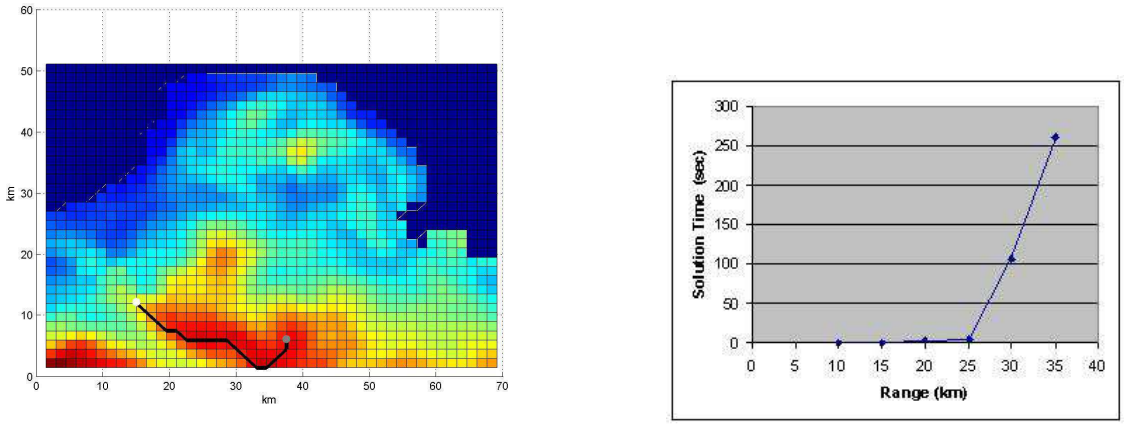

(a) (b)

Fig. 5. a) Result for single-vehicle case. Starting coordinates and range: $x = 15$km; $y = 12$km, $Range = 30$km; $Total\ \ Reward = 1489$ °C. b) Solution times for a single vehicle with starting position at $x = 15$km; $y = 12$km.

B. Results for Multi-Vehicle Case

Often times multiple vehicles are available which enables more thorough data collection in the region. It also brings some coordination issues such as avoiding vehicle collision and intelligent coordination of vehicles to cover as much critical regions as possible. The collision avoidance and coordination issues were handled by the introduction of Equation 24. Figures 6(a)–6(c) show paths generated for a two-vehicle case scenario as the vehicle path is gradually increased. As it can be observed from these figures the high

uncertainty regions are efficiently covered. The solution times are presented in Figure 6(d) which again increases exponentially as a function of path-points.

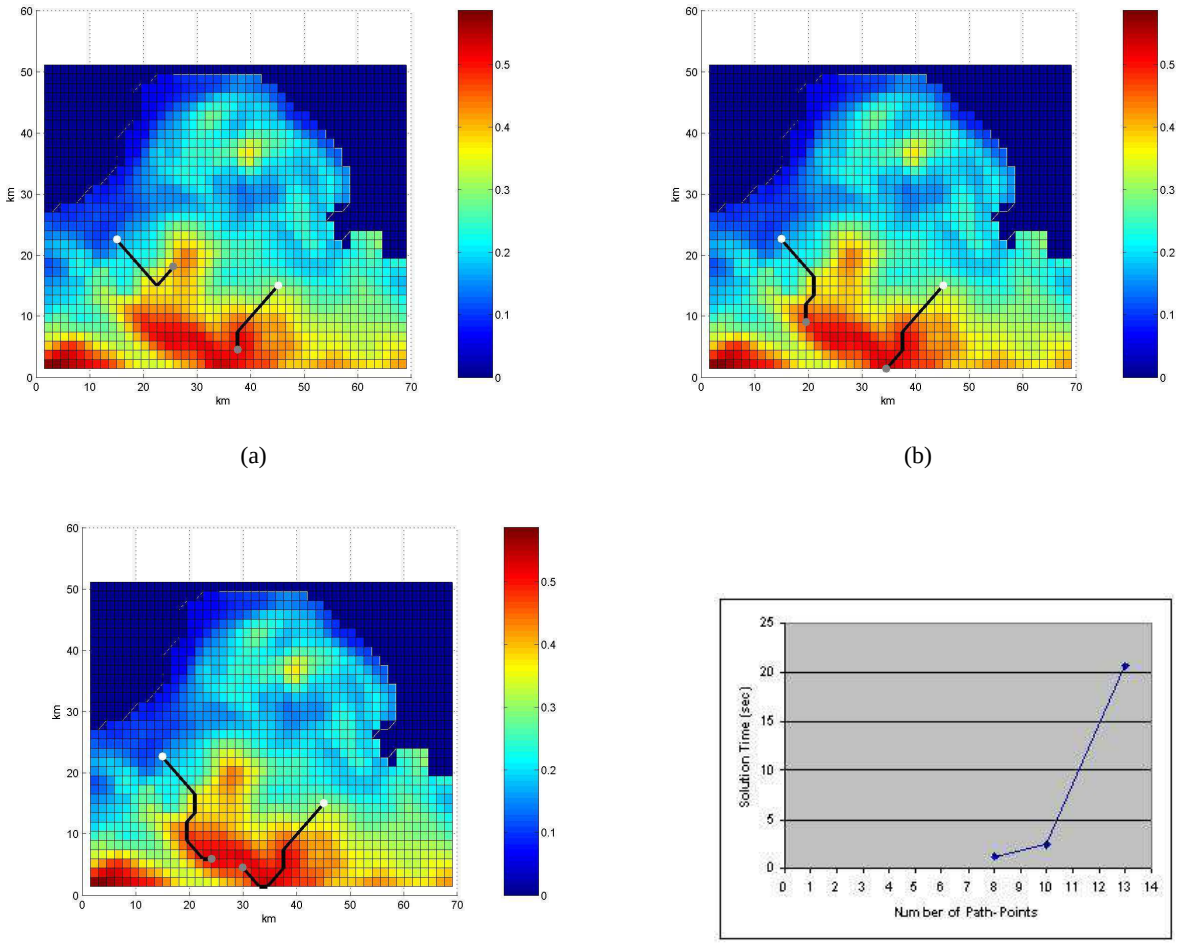

Fig. 6. a) Result for two-vehicle case. Starting coordinates and ranges: $x_1 = 15$km, $y_1 = 22.5$km, $Range_1 = 15$km; $x_2 = 45$km, $y_2 = 15$km, $Range_2 = 14$km; $Total\ \ Reward = 972$°C. b) Result for two-vehicle case. Starting coordinates and ranges: $x_1 = 15$km, $y_1 = 22.5$km, $Range_1 = 16.5$km; $x_2 = 45$km, $y_2 = 15$km, $Range_2 = 18$km; $Total\ \ Reward = 1273$ °C. c) Result for two-vehicle case. Starting coordinates and ranges: $x_1 = 15$km, $y_1 = 22.5$km, $Range_1 = 22.5$km; $x_2 = 45$km; $y_2 = 15$km, $Range_2 = 24$km; $Total\ \ Reward = 1879$ °C. d) Solution times for two vehicles with starting positions $x_1 = 15$km, $y_1 = 22.5$km ; $x_2 = 45$km; $y_2 = 15$km.

C. Vehicle Number Sensitivity

The aim of this section is to show the sensitivity of the solution time to the number of vehicles involved in the path planning task. We start with one vehicle and at each step introduce another vehicle until we reach five vehicles. Of course, each time a vehicle is added, a new global MILP optimization is carried out for all vehicles present. The path of all vehicles are optimized at once. The results are presented in Figures 7(a)–7(e). The solution times are presented in Figure **??**(f). There is a sudden increase as the number of vehicles increase. This behavior is in agreement with the exponential complexity of the problem. Note that in this illustration of the sensitivity to the number of vehicles, the starting points of vehicles are selected far apart from each other deliberately so that the addition of another vehicle does not affect the previous solution by much. This peculiar behavior allows more direct comparisons with previous illustrations.

D. Results with Ship Shadowing

As explained earlier, during a mission, AUVs are generally accompanied by a ship. The AUVs are dropped from the ship for their mission and dock to, or are collected by, the ship at the end. To handle this situation, extra constraints are added to the formulation. The constraints to be used depend on the type of communication (see Sect 4.D).

Figures 8(a)-(b) show two cases where the preferred mode of communication is chosen to be acoustical. Equations 26 and IV-D.1 are utilized in our formulation. The first case, where the defined proximity is set to be 15km takes 9sec to solve. When the proximity value is decreased to 9 the solution time also decreases to 5.25sec. The improvement is expected since tightening the constraint also shrinks the search space, resulting to strides in the solution time.

Another possible scenario is when the communication is via direct link in which case the AUVs do not need to stay in the vicinity of the ship throughout their mission, but must either park in some proximity of the ship or return to the ship at the end of their travel. This time Equations 28–29 are used. Figure 8(c) and Figure 8(d) present examples of the latter and former cases respectively. The region of proximity is defined to be 3km for Figure 8(c). The solution time is 2.3sec. For the case where AUVs need to return to the ship the solution time is 2.14sec.

VII. Time Progressive Path Planning

Up until this point, the sampling task had been assumed to take place in a single day without any pertinence to previous or following days. This is a perfectly fine scenario in rapid assessment in oceanography and it has been very successful for multiple uses at sea [6], [18]–[20], [48], [49]. However, a more sophisticated situation emerges when the sampling task has to be carried out over multiple days. In such time-evolving situations, the regions of high uncertainty are moving and transforming in shape as time progresses [4], [50] and the adaptive sampling fleet must adapt to the dynamic uncertainty field. In such scenarios, it is necessary to have some information exchange and coordination between the paths of the vehicles that are expected to be realized on consecutive days, so as to satisfy path optimality over both space and time.

Implementation a time dimension is introduced both for the primary and auxiliary variables. Every variable must have a new index that represents which day they belong to. The new objective function is then a summation of rewards from all days in consideration. A key point in establishing the link between consecutive days and introducing time-progressive features is to define the relation between the end path-point of vehicles on one day with the starting point on the following day. One option is to introduce the constraint that the starting point of the vehicle for a consecutive mission day should lie within a vicinity of the end point of the previous day. Another option is to impose the constraint that on consecutive mission days the vehicles should start their mission exactly at the end location of the previous day. This latter constraint can be defined as:

$\forall p \in [1, ..., P], \quad \forall d \in [2, ..., D]$:

$$x_{pd1} = x_{p(d-1)N_p} \tag{39}$$

$$y_{pd1} = y_{p(d-1)N_p} \tag{40}$$

where D stands for the total number of mission days. To further exemplify the inclusion of time dimension, the objective function can be written as:

Maximize

$$\sum_{p=1}^{P} \sum_{d=1}^{D} \sum_{k=1}^{N_p} f_{pdk} \tag{41}$$

The reader can see [35] for the full formulation for time progressive case. Assuming that AUVs have enough total range to complete sampling over the defined duration without any need to dock to get recharged and they continue their mission at the end point of the previous day, an example problem is solved whose results are presented in Figure 9. This example also reveals capabilities of the proposed formulation to find time global optimal solutions. The number of path-points chosen for both vehicles on both days is 8, which leads to a range of 15km per day. If we assume the absence of any information link between the uncertainty data for day 1 and day 2, looking at Figure 9(a), on day 1 the second vehicle, which starts its motion at x=45km and y=30km, would have needed to be close to the small peak located around x=40km, y=35km. With the 2-day information available, vehicle 2 moves on day1 such as shown on Figure 9(a). Since there is a constrained connection between day 1 and day 2, vehicle 2 compromises on the total amount of reward it can collect on day 1 ,and heads towards the high-uncertainty region that is predicted to form on day 2 around x=35km, y=10km. Over the two days, this enables the maximization of total reward, in the present case, the visit of high uncertainty regions.

The above discussion can be easily extended to $3-D$ case by simply adding an index for z coordinate to most of the variables involved in the formulation. This adds some new formulation variables related to the additional z coordinate and modifies the right-hand-sides of some of the inequalities.

VIII. Conclusions and discussions

In this paper we have addressed the problem of path planning of Autonomous Underwater Vehicles (AUVs) for adaptive sampling. We introduced an MILP based formulation which is capable of handling multi-vehicle and multi-day cases. Using MILP formulation techniques it is possible to successfully model all the constraints needed for different problem scenarios. The strength of the MILP formulation makes future problem formulation extensions and modifications possible. This point was exemplified within the *Autonomous Ocean Sampling Network (AOSN)* concept, (http://www.mbari.org/aosn/default.htm), [42].

We first developed the details of our optimization formulation, including the objective function and a wide range of constraints. Once formulated, we implemented and solved the problem using the XPress-MP optimization suit from “Dash optimization”. We preferred to use the native optimization formulation environment from Dash Optimization called Mosel to manage the formulation task. However, the formulation can be easily implemented with other optimization solver platforms. Using our new approach, we demonstrated a set of results for a wide range of scenarios using realistic ocean uncertainty fields. The effects of variations on the type of constraints, number of vehicles and time-dependence were studied and diverse sensitivity studies carried out. In all cases, the results show that the method is capable of generating desired solutions within allotted time limits.

The problem we study is an NP hard problem. Therefore, as the problem size increases the solution time increases exponentially. For the sizes we considered the solution time was short, especially in comparison to the time required to compute forecast ocean fields and their uncertainties. Our path planning results were obtained on Pentium 4, 2.8 GHz computer with 1 GByte of RAM. For larger problems, faster machines and grid/parallel computing are two options. The XPress-MP optimization suit we used already support parallel computing. i

There remain many directions for future research. For example, the correlation between the measurement performed at one location and the change of uncertainty values around that location as a result of the collected data, can been taken into direct consideration. In future work, we are planning to establish the link between a measurement performed at a generated path-point and its effect on uncertainty field or fields involved in the problem, including the Error Subspace Statistical Estimation (ESSE) technique into our optimization framework. Another line of research is the utilization of XML schemes [51] that control the parameters of our path planning schemes and couple the optimization with the ocean modeling and data assimilation schemes.

The framework we supplied can also be extended to be utilized at low-level path planning where linearized vehicle dynamics and some way-point information coming from high-level programming can

be combined to smoothen the path in an optimal manner. Another avenue of further research is the use of alternative solution techniques that can quickly generate suboptimal integer solutions and can warm-start the branch and bound algorithms. Candidate techniques include genetic algorithms and development of heuristics.

ACKNOWLEDGMENT

We thank the whole AOSN-II team and colleagues for their real-time work in Monterey Bay. Special thanks go P. J. Haley, W. G. Leslie, A. R. Robinson, N. Leonard, H. Schmidt and D. Paley for collaborations on ocean modeling and adaptive sampling. We also like to thank to Prof. D. Pucci De Farias and Prof. J. Leonard for the valuable discussions. This work was funded in part by the National Science Foundation (under ITR grant EIA-0121263) and the Department of Commerce (under NOAA - MIT Sea Grant College Program grant NA86RG0074). P. F. J. Lermusiaux was supported by the Office of Naval Research under grant N00014-05-1-0335, N00014-04-1-0534, N00014-05-G-0106 and N00014-05-1-0370.

REFERENCES

[1] M. Ehrendorfer, "Predicting the uncertainty of numerical weather forecasts: a review," *Meteorologische Zeitschrift*, vol. 4, pp. 47–183, 1997.

[2] P. F. J. Lermusiaux, "Data assimilation via error subspace statistical estimation, part ii: Middle atlantic bight shelfbreak front simulations and esse validation," *Monthly Weather Review*, vol. 127, no. 7, pp. 1408–1432, 1999.

[3] C. H. Bishop and Z. Toth, "Ensemble transformation and adaptive observations," *Journal of Atmospheric Sciences*, vol. 56, pp. 1748–1765, 1999.

[4] P. F. J. Lermusiaux, C. S. Chiu, G. G. Gawarkiewicz, P. Abbot, A. R. Robinson, R. N. Miller, P. J. Haley, W. G. Leslie, S. J. Majumdar, A. Pang, and F. Lekien, "Quantifying uncertainities in ocean predictions. refereed invited manuscript," *Oceanography, Special issue on "Advances in Computational Oceanography", T. Paluszkiewicz and S. Harper (Office of Naval Research), Eds.*, vol. 19, no. 1, pp. 92–105, 2006.

[5] C. H. Bishop, B. J. Etherton, and S. J. Majumdar, "Adaptive sampling with the ensemble transform Kalman filter. Part I: Theoretical aspects," *Monthly Weather Review*, vol. 129, pp. 420–436, 2001.

[6] A. R. Robinson and S. M. Glenn, "Adaptive sampling for ocean forecasting," *Naval Research Reviews*, vol. 51, no. 2, pp. 28–38, 1999.

[7] P. F. J. Lermusiaux, "Estimation and study of mesoscale variability in the strait of sicily," *Dynamics of Atmospheres and Oceans*, vol. 29, pp. 255–303, 1999.

[8] T. M. Hamill and C. Snyder, "Using improved background-error covariances from an ensemble Kalman filter for adaptive observations," *Monthly Weather Review*, vol. 130, pp. 1552–1572, 2002.

[9] P. F. J. Lermusiaux, P. Malanotte-Rizzoli, D. Stammer, J. Carton, J. Cummings, and A. M. Moore, "Progress and prospects of u.s. data assimilation in ocean research," *Oceanography, Special issue on "Advances in Computational Oceanography", T. Paluszkiewicz and S. Harper, Eds.*, vol. 19, no. 1, pp. 172–183, 2006.

[10] T. N. Palmer, J. Gelaro, J. Barkmeijer, and R. Buizza, "Singular vectors, metrics, and adaptive observations," *Journal of Atmospheric Sciences*, vol. 55, pp. 633–653, 1998.

[11] R. Gelaro, R. H. Langland, G. D. Rohaly, and T. E. Rosmond, "An assessment of the singular vector approach to targeted observations using the FASTEX data set," *Quarterly Journal of the Royal Meteorological Society*, vol. 125, pp. 3299–3328, 1999.

[12] R. Buizza and A. Montani, "Targeted observations using singular vectors," *Journal of Atmospheric Sciences*, vol. 56, pp. 1748–1765, 1999.

[13] T. Bergot, "Adaptive observations during FASTEX: A systematic survey of upstream flight," *Quarterly Journal of the Royal Meteorological Society*, vol. 125, pp. 3271–3298, 1999.

[14] R. H. Langland and G. D. Rohaly, "Adjoint-based targeting of observations for FASTEX cyclones," in *Reprints, Seventh Conference on Processes*. American Meteorology Society, 1996, pp. 369–371.

[15] N. L. Baker and R. Daley, "Observation and background adjoint sensitivity in the adaptive observation-targeting problem," *Quarterly Journal of the Royal Meteorological Society*, vol. 146, pp. 1431–1454, 2000.

[16] C. H. Bishop, C. A. Reynolds, and M. K. Tippett, "Optimization of the fixed global observing network in a simple model," *J. Atmos. Sci.*, vol. 60, 2003.

[17] S. J. Majumdar, C. H. Bishop, and B. J. Etherton, "Adaptive sampling with the ensemble transform Kalman filter. Part II: Field program implementation," *Monthly Weather Review*, vol. 130, pp. 1356–1369, 2002.

[18] P. F. J. Lermusiaux, "Estimation and study of mesoscale variability in the strait of sicily," *Dynamics of Atmospheres and Oceans*, vol. 29, pp. 255 –303, 1999.

[19] ——, "Evolving the subspace of the three-dimensional multiscale ocean variability: Massachusetts bay," *J. Marine Systems, Special issue on "Three-dimensional ocean circulation: Lagrangian measurements and diagnostic analyses"*, vol. 29, no. 1-4, pp. 385–422, 2001.

[20] ——, "Adaptive sampling, adaptive data assimilation and adaptive modeling." *Physica D., Refereed invited manuscript for a special issue on "Mathematical Issues and Challenges in Data Assimilation for Geophysical Systems: Interdisciplinary Perspectives", Christopher K.R.T. Jones and Kayo Ide, Eds.*, vol. 230, pp. 172–196, 2007.

[21] E. Fiorelli, N. E. Leonard, P. Bhatta, D. Paley, R. Bachmayer, and D. M. Fratantoni, "Multi-AUV control and adaptive sampling in monterey bay," in *Workshop on Multiple AUV Operations*, June 2004, pp. 134– 147.
[22] G. Laporte and S. Martello, "The selective travelling salesman problem," *Discrete Applied Mathematics*, vol. 26, pp. 193–207, 1990.
[23] E. Balas, "Prize collecting travelling salesman problem," *Networks*, vol. 19, pp. 621–636, 1989.
[24] B. L. Golden, L. Levy, and R. Vohra, "The orienteering problem," *Naval Research Logistics*, vol. 34, pp. 307–318, 1987.
[25] T. Schouwenaars, B. DeMoor, E. Feron, and J. How, "Mixed integer programming for safe multi-vehicle cooperative path planning." Porto, Portugal: EEC, September 2001.
[26] A. Richards, J. Bellingham, M. Tillerson, and J. How, "Coordination and control of multiple uavs," in *Proc. of the AIAA GNC*, Monterey, California, 5-8 August 2002, pp. Paper No. AIAA–2002–4588.
[27] A. R. Robinson, *"Forecasting and simulating coastal ocean processes and variabilities with the Harvard Ocean Prediction System", chapter in Coastal Ocean Prediction*, ser. AGU Coastal and Estuarine Studies Series. American Geophysical Union, 1999, pp. 77–100.
[28] P. F. J. Lermusiaux, "Uncertainty estimation and prediction for interdisciplinary ocean dynamics. refereed manuscript," *Journal of Computational Physics, Special issue of on "Uncertainty Quantification". J. Glimm and G. Karniadakis, Eds.*, pp. 176–199, 2006.
[29] P. F. J. Lermusiaux, A. R. Robinson, P. J. Haley, and W. G. Leslie, "Filtering and smoothing via error subspace statistical estimation," in *Advanced interdisciplinary data assimilation*, The OCEANS 2002 MTS/IEEE. Holland Publications, pp. 795–802.
[30] D. Guo, C. Evangelinos, and N. M. Patrikalakis, "Flow feature extraction in oceanographic visualization," ser. Computer Graphics International Conference, CGI, D. Cohen-Or, L. Jain, and N. Magnenat-Thalmann, Eds. Crete, Greece: Los Alamitos, CA: IEEE Computer Society Press, 2004., June 2004, pp. 162–173.
[31] D. Guo, "Automated feature extraction in oceanographic visualization," M.S. Thesis in Ocean Engineering, Massachusetts Institute of Technology, Cambridge, Massachusetts, February 2004.
[32] K. Heaney, G. Gawarkiewicz, T. Duda, and P. Lermusiaux, "Non-linear optimization of autonomous undersea vehicle sampling strategies for oceanographic data-assimilation," *Journal of Field Robotics. Special issue on Underwater Robotics*, vol. 24, no. 6, pp. 437–448, 2007.
[33] E. M. L. Beale and J. A. Tomlin, "Special facilities in a general mathematical programming system for non-convex problems using ordered sets of variables," in *Proceedings of the 5th International Conference on Operations Research*, J. Lawrence, Ed., Tavistock, London, 1969.
[34] H. P. Williams, *Model Building in Mathematical Programming*, 4th ed. John Wiley & Sons, Ltd, 1999.
[35] N. K. Yilmaz, "Path planning of autonomous underwater vehicles (AUVs) for adaptive sampling," Ph.D. dissertation, Massachusetts Institute of Technology, September 2005.
[36] D. Bertsimas and J. N. Tsitsiklis, *Introduction to Linear Optimization*. Athena Scientific, 1997.
[37] L. Freitag, M. Grund, C. von Alt, R. Stokey, and T. Austin, "A shallow water acoustic network for mine countermeasures operations with autonomous underwater vehicles." Underwater Defense Technology (UDT), 2005.
[38] H. Singh, J. G. Bellingham, F. H. S. Lemer, B. A. Moran, K. von der Heydt, and D. Yoerger, "Docking for an autonomous ocean sampling network," *IEEE Journal of Oceanic Engineering*, vol. 26, no. 4, pp. 498–514, 2001.
[39] J. J. Leonard, A. A. Bennett, C. M. Smith, and H. J. S. Feder, "Autonomous underwater vehicle navigation," Dept. of Ocean Engineering, Massachusetts Institute of Technology, Cambridge, MA, MIT Marine Robotics Laboratory Technical Memorandum, January 1998.
[40] M. S. L. Freitag, "Acoustic communications for regional undersea observatories," in *Proceedings of Oceanology International*, London, UK, March 2002, paper No. AIAA-2004-6530.
[41] I. F. Akyildiz, D. Pompili, and T. Melodia, "Challenges for efficient communication in underwater acoustic sensor networks," *C. ACM SIGBED Review*, vol. 1, no. 1, 2004.
[42] T. B. Curtin, J. G. Bellingham, J. Catipovic, and D. Webb, "Autonomous oceanographic sampling networks," *Oceanography*, vol. 6, no. 3, pp. 86–94, 1993.
[43] "Adaptive rapid environmental assessment (AREA): MIT, 2006," http://acoustics.mit.edu/faculty/henrik/uw_rto.html.
[44] D. E. Chang, J. E. M. S. Shadden, and R. Olfati-Saber, "Collision avoidance for multiple agent systems," in *Proc. CDC 42*, 2003, pp. 539–543.
[45] P. Ogren and N. E. Leonard, "A convergent dynamic window approach to obstacle avoidance," *IEEE Transactions on Robotics and Automation*, vol. 21, no. 2, pp. 188–195, April 2005.
[46] ——, "Obstacle avoidance in formation," in *Proc. of IEEE International Conference on Robotics and Automation*, 2003.
[47] ——, "A tractable convergent dynamic window approach to obstacle avoidance," in *Proc. IEEE/RSJ International Conference on Intelligent Robots and Systems (IROS)*, 2002.
[48] D. Wang, P. F. J. Lermusiaux, P. J. Haley, W. G. Leslie, and H. Schmidt, "Adaptive acoustical-environmental assessment for the focused acoustic field-05 at-sea exercise," in *Proceedings of IEEE/MTS Oceans'06 Conference*, no. 6pp, Boston, MA, 18-21 September 2006, pp. 175–187.
[49] D. Wang, P. Lermusiaux, P. Haley, W. Leslie, and H. Schmidt, "Adaptive acoustical-environmental assessment for the focused acoustic field-05 at-sea exercise," in *Proceedings of IEEE/MTS Oceans'06 Conference*, Boston, MA, 18-21 September 2006.
[50] P. F. J. Lermusiaux, "Uncertainty estimation and prediction for interdisciplinary ocean dynamics," *Journal of Computational Physics, Special issue on "Uncertainty Quantification", J. Glimm and G. Karniadakis, Eds., In press*, 2006, 24pp.
[51] C. Evangelinos, P. F. J. Lermusiaux, S. Geiger, R. C. Chang, and N. M. Patrikalakis, "Web-enabled configuration and control of legacy codes: An application to ocean modeling," *Ocean Modeling*, pp. 197–220, 2006.

Namik Kemal Yilmaz Dr. Namik Kemal Yilmaz received his B.S. degree in Mechanical Engineering with a minor in Computer Science from Middle East Technical University, Turkey. He pursued his graduate studies at MIT and received his M.S (2001) and Ph.D. (2005) degrees from the Mechanical Engineering Department. His research interest are in path planning, optimization, design and controls.

Constantinos Evangelinos Dr. Constantinos Evangelinos received his B.A. Honours in Mathematics from Cambridge University in 1993 and continued on to receive an Sc.M. (1994) and a Ph.D. (1999) from Brown University in Applied Mathematics. He is currently a Research Scientist in the Earth, Atmospheric and Planetary Sciences Department of MIT, where he works on Ocean State Estimation. His current research interests are in computational methods for variational as well as sequential data assimilation, adjoint techniques and automatic differentiation, parallel/grid computing approaches and performance modeling applied to grand challenge applications in the ocean sciences. He is a member of the IEEE Computer Society and the ACM.

Pierre F.J. Lermusiaux Dr. Pierre F.J. Lermusiaux is an Associate Professor of Mechanical Engineering at MIT. He obtained B.Eng./M.Eng. degrees (Highest honors and Jury's congratulations) from Liege University in 1992 and a Ph.D. in Engineering Sciences from Harvard in 1997. He has held Fulbright Foundation Fellowships, was awarded the Wallace Prize at Harvard in 1993, and presented the Ogilvie Young Investigator Lecture in Ocean Engineering at MIT in 1998. His current research interests include physical and interdisciplinary ocean dynamics, from sub-mesoscales to inter-annual scales. They involve physical-biogeochemical-acoustical ocean modeling, optimal estimation and data assimilation, uncertainty and error modeling, and the optimization of observing systems. He is a member of the Association of Engineers of Liege University, Friends of the University of Liege, Royal Meteorological Society, American Geophysical Union and Oceanography Society.

Nicholas Patrikalakis Dr. Nicholas M. Patrikalakis is the Kawasaki Professor of Engineering, Professor of Mechanical and Ocean Engineering, and Associate Head of the Department of Mechanical Engineering at MIT (http://me.mit.edu/people/personal/nmp.htm). He received a Diploma in Naval Architecture and Mechanical Engineering in 1977 from the National Technical University of Athens, Greece, and a Ph.D. in Ocean Engineering in 1983 from MIT. His current research interests include: shape similarity evaluation, marine robotics and distributed information systems for multidisciplinary ocean behavior forecasting. He is a member of ACM, ASME, CGS, IEEE, ISOPE, SIAM, SNAME and TCG, and he is editor, co-editor, or member of the editorial board of six international journals (CAD, JCISE, IJSM, TVC, GM, IJAMM). He has served as program chair of CGI '91, program co-chair of CGI '98, Pacific Graphics '98, ACM Solid Modeling Symposium 2002, general co-chair of the ACM Solid Modeling Symposium 2004, and general Convention Chair for the 2005 Convention on Shapes and Solids (ACM SPM'05 and SMI'05).

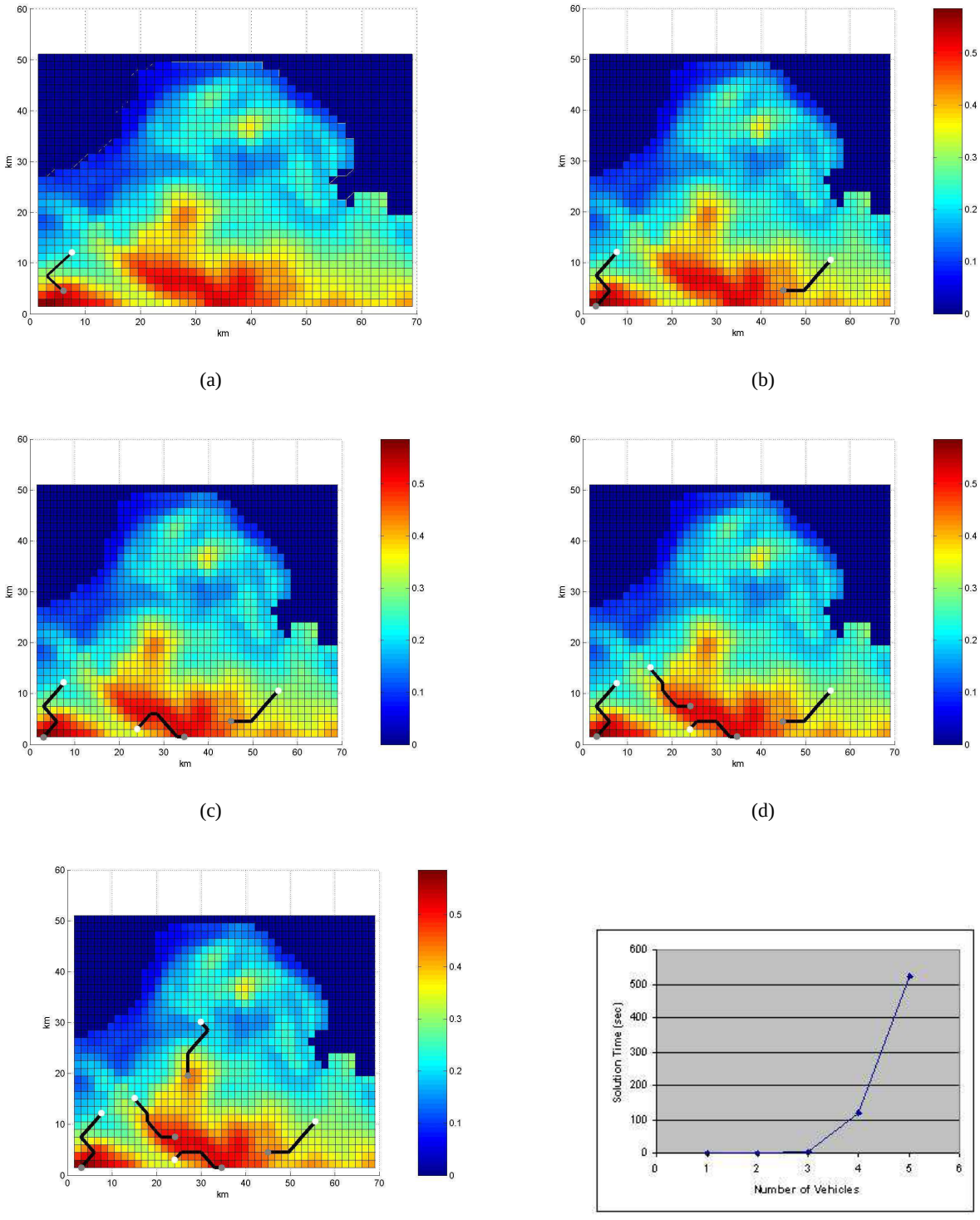

(a) (b) (c) (d) (e) (f)

Fig. 7. a) Result for single-vehicle case. Starting coordinates: $x_1 = 7.5$km, $y_1 = 8$km, $Range_1 = 15$km. b) Result for two-vehicle case. Starting coordinates: $x_1 = 7.5$km, $y_1 = 8$km, $Range_1 = 15$km; $x_2 = 55.5$km, $y_2 = 10.5$km, $Range_2 = 13$km. c) Result for three vehicle case. Starting coordinates: $x_1 = 7.5$km, $y_1 = 8$km, $Range_1 = 15$km; $x_2 = 55.5$km, $y_2 = 10.5$km, $Range_2 = 13$km; $x_3 = 24$km, $y_3 = 3$km, $Range_3 = 13.5$km. d) Result for four vehicle case. Starting coordinates: $x_1 = 7.5$km, $y_1 = 8$km, $Range_1 = 15$km; $x_2 = 55.5$km, $y_2 = 10.5$km, $Range_2 = 13$km; $x_3 = 24$km, $y_3 = 3$km, $Range_3 = 13.5$km; $x_4 = 15$km, $y_4 = 15$km, $Range_4 = 13$km. e) Result for five vehicle case. Starting coordinates: $x_1 = 7.5$km, $y_1 = 8$km, $Range_1 = 15$km; $x_2 = 55.5$km, $y_2 = 10.5$km, $Range_2 = 13$km; $x_3 = 24$km, $y_3 = 3$km, $Range_3 = 13.5$km; $x_4 = 15$km, $y_4 = 15$km, $Range_4 = 13$km; $x_5 = 30$km, $y_5 = 30$km, $Range_5 = 13$km. f) Solution times as a function of number of vehicles in the fleet.

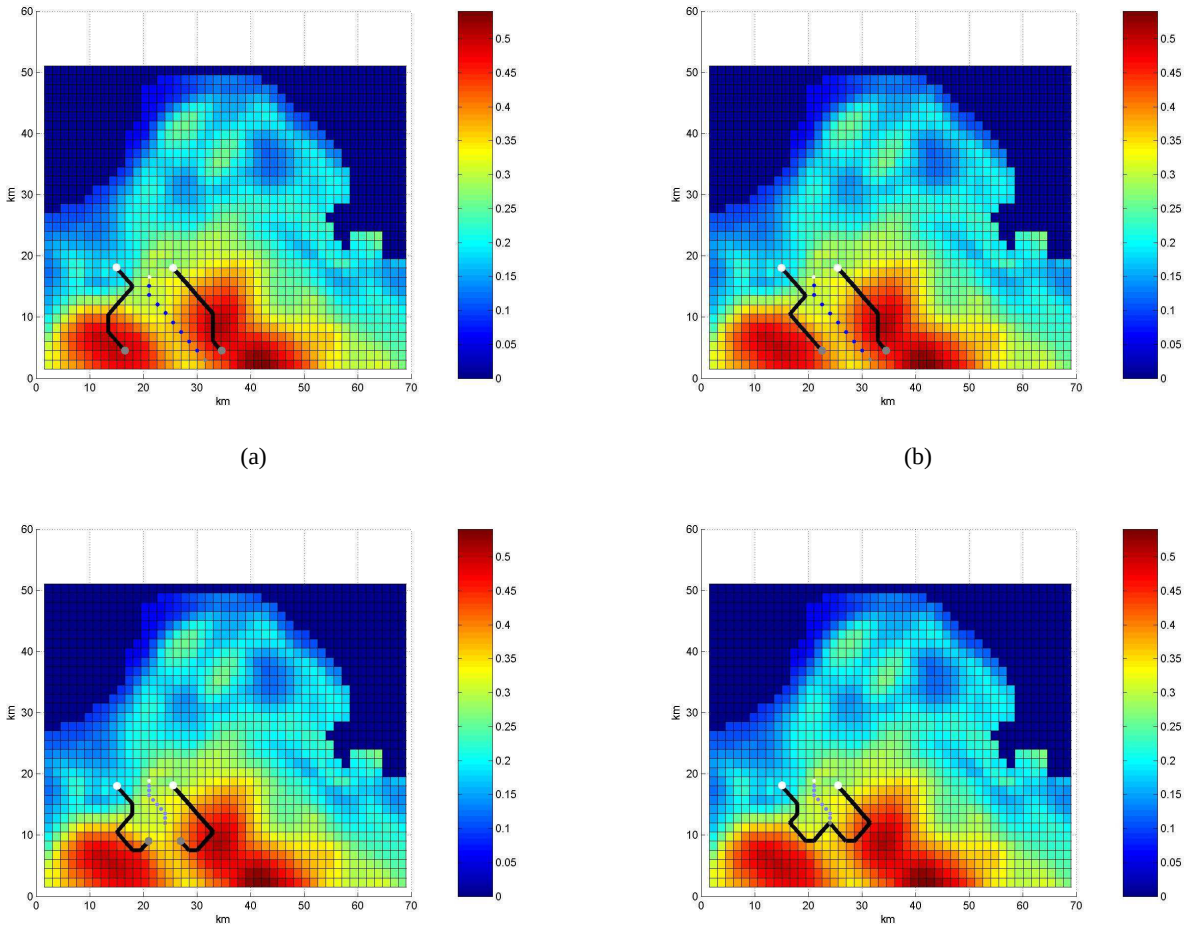

Fig. 8. a) Results for two vehicles shadowed by a ship for the case where AUVs must be in 15km vicinity of the ship. Ship path is shown with dotted line. Starting coordinates: $x_1 = 15$km, $y_1 = 18$km, $Range_1 = 19$km; $x_2 = 25.5$km, $y_2 = 18$km, $Range_2 = 18$km. b) Results for two vehicles shadowed by a ship for the case where AUVs must be in 9km vicinity of the ship. Ship path is shown with dotted line. Starting coordinates: $x_1 = 15$km, $y_1 = 18$km, $Range_1 = 19$km; $x_2 = 25.5$km, $y_2 = 18$km, $Range_2 = 18$km. c) Results for two vehicles shadowed by a ship for the case where the end path-points of AUVs must be in 3km vicinity of the ship. Ship path is shown with dotted line. Starting coordinates: $x_1 = 15$km, $y_1 = 18$km, $Range_1 = 19$km; $x_2 = 25.5$km, $y_2 = 18$km, $Range_2 = 18$km. d) Results for two vehicles shadowed by a ship for the case where the AUVs must return to the ship. Ship path is shown with dotted line. Starting coordinates: $x_1 = 15$km, $y_1 = 18$km, $Range_1 = 19$km; $x_2 = 25.5$km, $y_2 = 18$km, $Range_2 = 18$km.

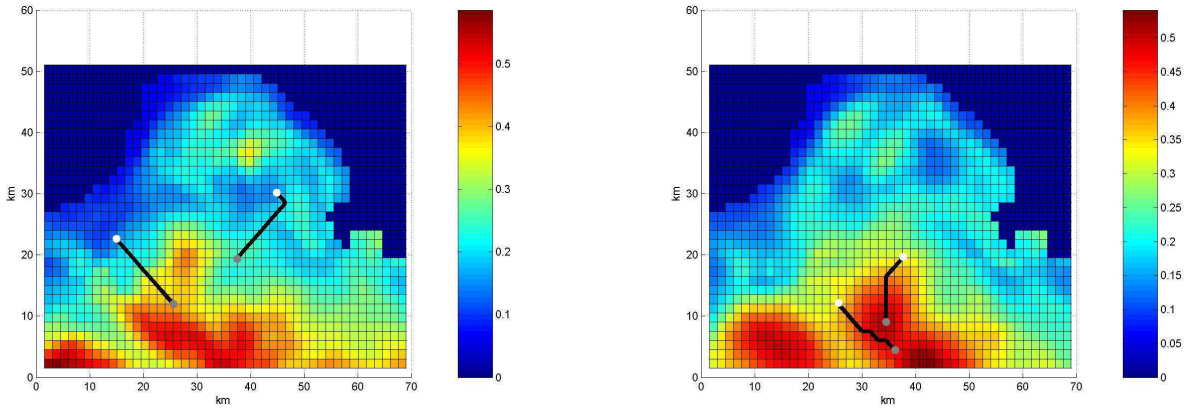

(a) (b)

Fig. 9. a) Results for first day of a time-progressive case example. Starting coordinates: $x_1 = 15$km, $y_1 = 22.5$km, $Range_1 = 15$km; $x_2 = 45$km, $y_2 = 30$km, $Range_2 = 15$km. b) Results for second day of a time-progressive case example. Starting coordinates: $x_1 = 25.5$km, $y_1 = 12$km, $Range_1 = 13.5$km; $x_2 = 37.5$km, $y_2 = 19.5$km, $Range_2 = 12$km.